ChemComm

ROYAL SOCIETY OF CHEMISTRY

COMMUNICATION

View Article Online
View Journal | View Issue

Check for updates

Cite this: *Chem. Commun.*, 2024, **60**, 8063

Received 24th March 2021,
Accepted 1st June 2021

DOI: 10.1039/d1cc01596f

rsc.li/chemcomm

Synergistic catalysis: cobalt-catalyzed cascade reaction for the oxidative cleavage of olefins to access esters†

Xiangzhu Yu, Zhengjia Zhao, Shangzhi Tan, Lina Zhu, Weiru Fu, Yue An* and Lianyue Wang *

An efficient strategy for the oxidative cleavage of C═C bonds in olefins to form esters with one or multiple carbon atoms less over heterogeneous cobalt/nitrogen-doped carbon catalyst with dioxygen as the oxidant was described. The protocol features a wide substrate range including the challenging inactive aliphatic and long-chain alkyl aryl olefins. The reactivity of the catalyst did not decrease after reused for seven times. Characterization and control experiments reveal that synergistic effects between the metallic Co nanoparticles and Co–N$_x$ sites provide access to the excellent catalytic activity.

Selective oxidative cleavage of olefins to the carbonyl compounds is a very important transformation in the field of organic synthesis.[1] The ozonolysis reaction and Lemieux–Johnson oxidation reaction are the traditional oxidation method for the C═C bond cleavage, which use the toxic and expensive O_3 and osmium tetroxide as oxidants.[2] Other oxidants, such as $KMnO_4$, PhIO/HBF_4, and $NaIO_4$ generated stoichiometric amounts of waste, which limits their sustainable applications.[3] Oxygen is an oxidant of choice from the perspective of abundance, safety and cheapness. A number of reports on the homogeneous transition-metal and metal-free catalysts for the aerobic oxidative cleavage of C═C bonds in olefins have been well developed.[1c,4] These catalytic systems still have some inherent drawbacks such as no reusability of the catalyst. Furthermore, addition of ligands, organic bases, and other promoters complicates the separation process of the reaction.[5] Heterogeneous catalysis has the advantages of simple post-treatment process and recyclable catalyst. However, heterogeneous catalysts are rarely used to catalyze the breaking of C═C bond due to the limitation of low catalytic activity in general. Some noble metal heterogeneous catalysts (such as Pt, Ru and Au) were used for the oxidative cleavage of C═C bond.[6] Iron-based non-noble metal heterogeneous catalysts have also been developed, however, they exhibited limited substrate scope and low product selectivity.[7] Although homogeneous and heterogeneous metal catalysts as well as other metal-free systems have been applied to the C═C bond cleavage, most of them are still suffering from limited substrate range and low product selectivity. Some catalyst systems can achieve C═C bond cleavage of non-active alkyl olefin,[8] but it has not been reported successive cleavage adjacent C–C single bond in addition to the breaking of C═C bonds in olefins. In addition, the cleavage products are aldehydes or acids (Scheme 1). The direct formation of esters by oxidative cleavage of C═C bonds is still unknown. Therefore, the development of an efficient and recyclable heterogeneous non-noble metal catalyst for the aerobic oxidative cleavage and esterification of C═C bonds is imperative, which will be an important complement to the oxidative cleavage of C═C bonds.

Recently, we demonstrated the use of heterogeneous nitrogen-doped carbon-based cobalt catalysts for the oxidative cleavage of C(OH)–C bond to access esters and Wacker-type oxidation of olefins. In this regard, cobalt nanoparticles are responsible for the cleavage of C–C bonds in alcohols,[9] while single atom cobalt is the active centre for the Wacker-type oxidation.[10] It is well known that metal–NC materials obtained by high-temperature pyrolysis method usually include graphene encapsulated metal nanoparticles and metal–N$_x$ sites.[11] Hence, we envisaged that metal–NC catalyst can realize cascade reaction for the oxidative cleavage of olefins to esters by synergistic cobalt nanoparticles and Co–N$_x$. To the best of our knowledge, the synergistic catalysis by

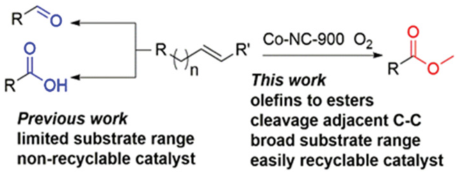

Scheme 1 Successive C═C bond cleavage of olefins.

College of Chemistry and Chemical Engineering, Liaoning Normal University, Huanghe Road 850#, Dalian 116029, P. R. China.
E-mail: lianyuewang@lnnu.edu.cn, anyue_11@163.com

† Electronic supplementary information (ESI) available: Catalyst preparation, characterization and control experiment. See DOI: 10.1039/d1cc01596f

heterogeneous cobalt-based catalyst, for the first time, was applied in the functionalization of C=C bonds by oxidative cleavage.

In this work, we describe an efficient strategy for the cleavage of C=C bonds in olefins to form esters over heterogeneous cobalt/N-doped carbon catalyst with dioxygen as the oxidant. The catalytic system showed a wide substrate range including the challenging inactive aliphatic and long-chain alkyl aryl olefins. The ability to successive cleavage adjacent C–C single bond in addition to the breaking of C=C bonds is significant feature compared to the previous reports. The catalyst could be reused seven times without obvious loss in activity. Characterization and control experiments reveal that synergistic effects between the metallic Co nanoparticles and Co–N_x sites in the Co–NC-900 catalyst provide access to the excellent catalytic activity.

The catalyst preparation process follows our previous method with a slight modification (see the ESI†). The obtained catalysts from different pyrolysis temperatures are labelled as Co–NC-*X* (*X* stands for pyrolysis temperature).[9]

Styrene (**1a**) was used as the model substrate to evaluate the esterification performance of Co–NC-*X* catalysts (Table 1). The blank experiment showed that olefin esterification could not be carried out without catalysts Co–NC-*X* (Table 1, entry 1). Pyrolysis temperature has a great influence on the catalytic activity (Table 1, entries 2–5). The evaluation results showed that the catalytic performance of Co–NC-900 was the best (Table 1, entry 2). Using the $Co(OAc)_2·4H_2O$ or complexes of $Co(OAc)_2·4H_2O$ and 1,10-phenanthroline as catalysts, the target products were obtained in 5% and 9%, respectively (Table 1, entries 6 and 7). The main by-products are 1-phenyl ethanol and acetophenone. NC-900 catalyst prepared from sucrose and melamine only gave 10% yield of **2a** (Table 1, entry 8), indicating that the surviving cobalt species after acid treatment play a crucial role in this transformation. The yield of **2a** is reduced to 68% when air was used instead of oxygen as the oxidant. No target product was detected in the N_2 atmosphere, which proved that O_2 was crucial to achieve this transformation (Table 1, entries 9 and 10). When the amount of K_2CO_3 was reduced to 5%, the yield of the **2a** was significantly decreased with (1-methoxyethyl)benzene as the major by-product (Table 1, entry 11). In the absence of K_2CO_3, the yield of **2a** is only 9% (Table 1, entry 12), suggesting that K_2CO_3 is necessary for this transformation. Then the other bases were also studied (Table S1, ESI†), the results showed that K_2CO_3 was the best choice. The decrease of temperature and pressure led to a slight decrease in **2a** yield (Table 1, entries 13 and 14), indicating that suitable temperature and pressure are important conditions for efficient conversion. The amount of catalyst was increased to 10 mol%, and 96% of **2a** was obtained (Table 1, entry 15). When the template SiO_2 was retained, 47% of **2a** was obtained (Table 1, entry 16), indicating that the mesoporous structure can greatly improve the catalytic activity. The yield of the target product in the gram-scale experiment was 70% (Table 1, entry 17).

The heterogeneous nature of the Co–NC-900 catalyst was determined by hot-filtration experiment. After 6 h of reaction, the catalyst was filtered out, and the filtrate continued to react but no further formation of the target product was detected (Fig. S2, ESI†). The stability of the catalyst was studied. The results showed that the catalyst could be reused for seven times, and the reaction activity did not decrease (Fig. S3, ESI†). The recovered catalyst was characterized by XRD and HRTEM (Fig. S4, ESI†). The results showed that the structure and composition of the recovered catalyst did not change significantly compared with that of the fresh catalyst, indicating that the catalyst had excellent stability.

The N_2 adsorption–desorption characterization of the catalyst Co–NC-900 proved the existence of mesoporous structure (Fig. S5, ESI†). The X-ray diffraction pattern (XRD) show the diffraction peaks of 44.2° and 51.5° (Fig. S6, ESI†), which indicated the lattice planes (111 and 200) of metal cobalt (JCPDS no. 15-0806). Raman spectra show that Co–NC-900 possesses more N-doped atoms and less graphitic crystallites at the edges of the mesoporous nanocarbon, which is benefit for the increase of catalytic activity (Fig. S7, ESI†).[12] The structure and morphology of Co–NC-900 were observed by scanning electron microscopy (SEM) and transmission electron microscopy (TEM). The catalyst had honeycomb mesoporous structure (Fig. S8, ESI†). The highlights of the Bed-C mode (Fig. 1a) and the TEM (Fig. 1b) can show that there were surviving cobalt nanoparticles with a size of 5–20 nm after acid leaching. High-resolution transmission electron microscopy (HRTEM) showed the presence of metal Co species with lattice spacing of 0.2 nm and 0.17 nm, which was consistent with the Co (111) and (200) planes in XRD (Fig. 1c). The energy-dispersive X-ray (EDX) elemental mapping showed that C, N, O and Co elements were uniformly distributed in the catalyst (Fig. 1d).

The results of X-ray photoelectron spectroscopy (XPS) show that there are mainly C, N, O and Co elements in the Co–NC-900

Table 1 Optimization of the reaction conditions[a]

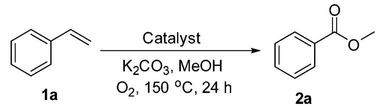

Entry	Catalysts	Conv.[b] [%]	Yield[b] [%]
1	—	10	—
2	Co–NC-900	98	89
3	Co–NC-800	95	77
4	Co–NC-700	95	63
5	Co–NC-600	94	45
6	$Co(OAc)_2·4H_2O$	36	5
7	$Co(OAc)_2·4H_2O$/1,10-phen	99	9
8	NC-900	42	10
9[c]	Co–NC-900	96	68
10[d]	Co–NC-900	37	—
11[e]	Co–NC-900	92	39
12[f]	Co–NC-900	29	9
13[g]	Co–NC-900	99	73
14[h]	Co–NC-900	97	60
15[i]	Co–NC-900	99	96
16	$Co(phen)_2(OAc)_2@SiO_2$-900	99	47
17[j]	Co–NC-900	99	70

[a] Reaction conditions: **1a** (0.25 mmol), K_2CO_3 (20 mol%), catalyst (7.5 mol%), MeOH (4 mL), 0.6 MPa O_2, 150 °C, 24 h. [b] Conversion and yield were determined by GC using biphenyl as the internal standard. [c] Air. [d] N_2. [e] 5 mol% K_2CO_3. [f] Without K_2CO_3. [g] 130 °C. [h] 0.4 MPa O_2. [i] 10 mol% catalyst. [j] **1a** (10 mmol, 1.04 g), catalyst (5 mol%), MeOH (15 mL), 72 h.

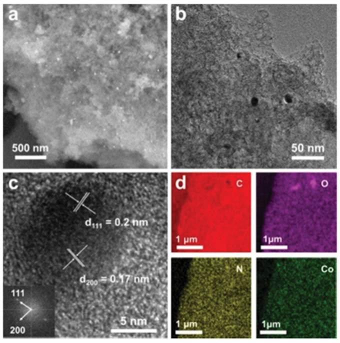

Fig. 1 Microstructure observation for Co–NC-900. (a) SEM images under BED-C mode. (b) TEM image and (c) HRTEM image. (d) Elemental mapping images.

(Fig. S11, ESI†). High resolution N1s spectra show four types of peaks, corresponding to pyridine nitrogen or Co–N (398.7 eV), pyrrole nitrogen (399.8 eV), graphitized nitrogen (400.8 eV) and nitrogen oxide (403.9 eV) (Fig. S11c, ESI†).[13] Compared with the catalyst at 600–800 °C pyrolysis temperature, the graphitized nitrogen content of Co–NC-900 is the highest (Table S2, ESI†), which is consistent with the results of Raman spectroscopy. In the high-resolution Co2p spectrum, the peak of 778.2 eV marked as zero-valent Co,782.3 eV belongs to the Co component of Co–N_x configuration (Fig. S11d, ESI†).[14]

Nitrogen-doped carbon-supported metal materials formed by high temperature pyrolysis usually include metal–N_x and metal nanoparticles. In the present Co–NC-900, XPS shows that Co–N_x exists in the catalyst, and the HRTEM shows that graphene-coated cobalt nanoparticles are distributed on the surface of the catalyst. Therefore, it is necessary to judge the real active sites for catalytic esterification of olefins. In order to determine whether Co–N_x is playing a role, KSCN control experiment was carried out under the standard conditions (Fig. 2). There was no effect in the yield after adding the binding molecule KSCN. We reduced the amount of catalyst to 3.0 mol% from the point of view of kinetics. When no KSCN was added, **2a** was obtained in 60% yield. In the presence of KSCN, the yield of **2a** was significantly decreased to 30%. When styrene was used as the substrate and isopropanol was used as the solvent, the yield of **3b** is significantly reduced. When **3a** was used as the substrate, the yield of ester increased slightly in the presence of KSCN. In addition, the negative correlation between the content of Co–N_x and the yield of products was observed (Fig. S12, ESI†). These results were completely consistent with our previous results.[9,10] That is, Co–N_x was the active center for the Wacker-type oxidation of olefin, and cobalt nanoparticles cleaved the C–C bonds in alcohols or ketones to form esters. Therefore, we confirm that Co–NC catalyst can realize cascade reaction for the oxidative cleavage of olefins to access esters by synergistic cobalt nanoparticles and Co–N_x sites.

After the optimum reaction conditions obtained, the substrate range of olefin was continued to be explored (Table 2). The results showed that olefin derivatives were successfully converted to the corresponding esters in moderate to good yields (**2b–2n**). The Olefins containing heterocycles or naphthalene rings were also converted successfully, giving the products in 55% and 60% (**2o**, **2p**). The long-chain alkyl aryl olefin **1q** could give 52% yield of corresponding ester. More challenging inactive aliphatic olefins were also studied. The results showed that the catalytic system could be efficient successive cleavage of adjacent –$(C–C)_n$– apart from the cleavage of C=C bonds, affording the corresponding esters in moderate yields (**1r–1t**). In addition, cinnamates (**1u**, **1v**) were also suitable substrates for this transformation. The α,β-unsaturated ketone (**1w–1y**) was investigated and found that no matter whether it contains a substituent, it can also undergo smoothly cleavage of C=C bond. The *trans*-stilbene (**1z**) obtained **2a** with yield of 81%. Drug intermediate (**2q**) can be obtained after the oxidative cleavage of **1aa**.

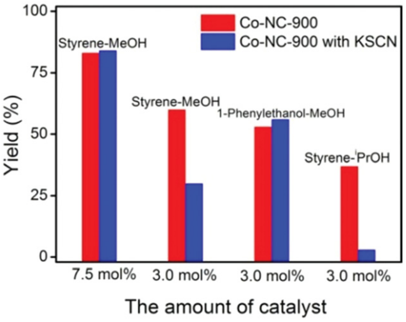

Fig. 2 KSCN control experiments. Reaction conditions: reactant (0.25 mmol), K_2CO_3 (20 mol%), MeOH (4 mL), 0.6 MPa O_2, 150 °C,24 h.

The free radical inhibition experiment showed that the reaction might not involve the free radical reaction (Scheme S1, ESI†). Styrene (**1a**) was selected as an example to track the time of olefin oxidation (Fig. S13, ESI†). **3a** and **3b** were detected by GC–MS, indicating that they might be intermediates. When **3a** and **3b** were used as substrates under the standard conditions, the yields of **2a** were obtained in 88% and 91% (Table S3, ESI†). When **3c** used as substrate, the main product was tertiary alcohol, which cannot be oxidized to ketone and no esters can be formed. **3d** was also detected by GC–MS and was unable to undergo oxidative cleavage to esters indicating that **3d** was not intermediate but by-product. The above results showed that **3b** was a very critical intermediate. Based on our previous research,[10] a series of reactions took place next in **3b**, and finally the target product would be obtained. Although **3e** was not detected, **it** can be quickly converted into products. On the basis of the catalyst characterization and control experiment results and pertinent literature reports, a possible reaction mechanism was proposed (Scheme S2, ESI†). First, **1a** undergoes Wacker oxidation to obtain **3b** catalyzed by Co–N_x. Next, **3b** undergoes sequence reaction involves stepwise oxidation/nucleophilic addition/C–C bond cleavage. During the cleavage of the C–C bond, formic acid was released and decomposed into CO_2 and H_2 (Fig. S14–S16, ESI†).

In conclusion, we reported an efficient oxidative cleavage and functionalization of C=C bonds of olefins to access eaters, *via* cascade reactions promoted by heterogeneous cobalt/N-doped carbon catalyst. A broad range of olefins including simple styrene, α,β-unsaturated ketones, the challenging inactive aliphatic and long-chain alkyl aryl olefins undergo successfully to the corresponding esters with one or multiple carbon atoms shorter.

Table 2 Substrate scope of olefins[a]

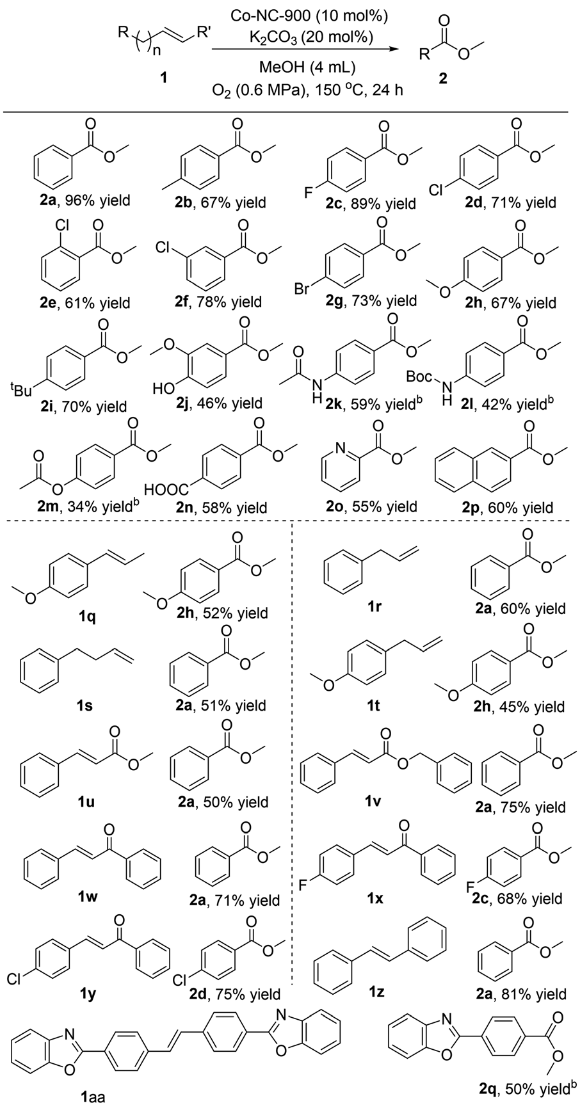

[a] Reaction conditions: **1** (0.25 mmol), K_2CO_3 (20 mol%), catalyst (10 mol%), MeOH (4 mL), 0.6 MPa O_2, 150 °C. Yield was determined by GC using biphenyl as the internal standard. [b] Determined by NMR.

Catalyst characterization and control experiments disclosed that synergistic catalysis on Co nanoparticles and Co–N_x site is indeed responsible for the excellent catalytic activity. Preliminary mechanistic research showed that the reaction process underwent a cascade reaction. This work not only expands the application field of nitrogen-doped carbon materials, but also provides a new way for the oxidative cleavage of C=C bonds.

Financial support from the Department of Science and Technology of Liaoning Province (No. 2019-ZD-0470), the National Natural Science Foundation of China (No. 21773227) and the State Key Laboratory of Catalysis in DICP (No. N-20-11).

Conflicts of interest

There are no conflicts to declare.

Notes and references

1 (*a*) C. J. Allpress and L. M. Berreau, *Coord. Chem. Rev.*, 2013, **257**, 3005; (*b*) B. M. Trost and C. J. Li, *Modern Alkyne Chemistry Catalytic and Atom-Economic Transformations*, Wiley-VCH, Germany, 2014; (*c*) U. Garaz, S. Raul and D. Esther, *ACS Catal.*, 2017, **7**, 3050.

2 (*a*) V. Balzani, A. Credi and M. Venturi, *ChemSusChem*, 2008, **1**, 26; (*b*) R. Pappo, D. S. Allen, R. U. Lemieux and W. S. Johnson, *J. Org. Chem.*, 1956, **21**, 478.

3 (*a*) D. J. Sam and H. E. Simmons, *J. Am. Chem. Soc.*, 1972, **94**, 4024; (*b*) K. Miyamoto, N. Tada and M. Ochiai, *J. Am. Chem. Soc.*, 2007, **129**, 2772; (*c*) G. K. Dewkar, S. V. Narina and A. Sudalai, *Org. Lett.*, 2003, **5**, 4501.

4 (*a*) T. Wdowik and S. R. Chemler, *J. Am. Chem. Soc.*, 2017, **139**, 9515; (*b*) R. Lin, F. Chen and N. Jiao, *Org. Lett.*, 2012, **14**, 4158; (*c*) Y. Deng, X. Wei, H. Wang, Y. Sun, T. Noel and X. Wang, *Angew. Chem., Int. Ed.*, 2017, **56**, 832; (*d*) T. Wang and N. Jiao, *J. Am. Chem. Soc.*, 2013, **135**, 11692; (*e*) J. Li, J. Wei, B. Zhu, T. Wang and N. Jiao, *Chem. Sci.*, 2019, **10**, 9099.

5 (*a*) A. Gonzalez-de-Castro and J. Xiao, *J. Am. Chem. Soc.*, 2015, **137**, 8206; (*b*) J. Eriksen and C. S. Foote, *J. Am. Chem. Soc.*, 2002, **102**, 6083; (*c*) A. Wang and H. Jiang, *J. Org. Chem.*, 2010, **75**, 2321.

6 (*a*) H. Hong, L. Hu, M. Li, J. Zheng, X. Sun, X. Lu, X. Cao, J. Lu and H. Gu, *Chemistry*, 2011, **17**, 8726; (*b*) W.-K. Wong, X.-P. Chen, T.-W. Chik, W.-Y. Wong, J.-P. Guo and F.-W. Lee, *Eur. J. Inorg. Chem.*, 2003, 3539; (*c*) M. Turner, V. B. Golovko, O. P. Vaughan, P. Abdulkin, A. Berenguer-Murcia, M. S. Tikhov, B. F. Johnson and R. M. Lambert, *Nature*, 2008, **454**, 981.

7 (*a*) L. Hadian-Dehkordi and H. Hosseini-Monfared, *Green Chem.*, 2016, **18**, 497; (*b*) M. J. Rak, M. Lerro and A. Moores, *Chem. Commun.*, 2014, **50**, 12482.

8 X. Baucherel, J. Uziel and S. Juge, *J. Org. Chem.*, 2001, **66**, 4504.

9 H. Luo, L. Wang, S. Shang, G. Li, Y. Lv, S. Gao and W. Dai, *Angew. Chem., Int. Ed.*, 2020, **59**, 19268.

10 G. Huang, L. Wang, H. Luo, S. Shang, B. Chen, S. Gao and Y. An, *Catal. Sci. Technol.*, 2020, **10**, 2769.

11 (*a*) X. Li, A. E. Surkus, J. Rabeah, M. Anwar, S. Dastigir, H. Junge, A. Bruckner and M. Beller, *Angew. Chem., Int. Ed.*, 2020, **59**, 15849; (*b*) A. Zitolo, V. Goellner, V. Armel, M. T. Sougrati, T. Mineva, L. Stievano, E. Fonda and F. Jaouen, *Nat. Mater.*, 2015, **14**, 937.

12 S. Shang, W. Dai, L. Wang, Y. Lv and S. Gao, *Chem. Commun.*, 2017, **53**, 1048.

13 (*a*) S. Pylypenko, S. Mukherjee, T. S. Olson and P. Atanassov, *Electrochim. Acta*, 2008, **53**, 7875; (*b*) C. Yang, L. Fu, R. Zhu and Z. Liu, *Phys. Chem. Chem. Phys.*, 2016, **18**, 4635.

14 L. He, F. Weniger, H. Neumann and M. Beller, *Angew. Chem., Int. Ed.*, 2016, **55**, 12582.